Ground Effects in FAA's Integrated Noise Model

Gregg G. Fleming[a)], Joseph Burstein[b)], Amanda S. Rapoza[c)], David A. Senzig[d)], John M. Gulding[e)]

[a), b), c), d)] United States Department of Transportation
John A. Volpe National Transportation Systems Center, Acoustics Facility
Kendall Square
Cambridge, MA 02142

[e)] United States Department of Transportation
Federal Aviation Administration, Office of Environment and Energy, AEE-120
800 Independence Avenue
Washington, D.C. 20591

The lateral attenuation algorithm in the Federal Aviation Administration's (FAA) Integrated Noise Model (INM) has historically been based on the two regression equations described in the Society of Automotive Engineers' (SAE) Aerospace Information Report (AIR) 1751. These equations, which together represent a single relationship developed from measured data for 1960s and 1970s aircraft with low-bypass ratio jet engines, are applied equally in INM to the entire aircraft fleet. Further, these equations cannot take into account the effects of propagation over acoustically hard terrain, such as water. Consequently, in 1997 the INM development team initiated the task of revising the lateral attenuation algorithm within the model. The primary component of the revised algorithm is an entirely new methodology for considering ground effects. The methodology, which is based upon a newly-compiled spectral data base, along with the physical acoustics model of Embleton, Piercy and Daigle, will exist in INM as a library of regression equations. As such, this approach will offer the accuracy and flexibility of a pure physical acoustics model, coupled with relatively modest computer runtimes. This paper documents the scientifically-founded and experimentally-validated approach to computing ground effects slated for inclusion in INM.

Primary subject classification: 76.1; Secondary subject classification: 24.9

1. INTRODUCTION

The lateral attenuation algorithm in the Federal Aviation Administration's (FAA) Integrated Noise Model (INM) has historically been based on regression equations described in the Society of Automotive Engineers' (SAE) Aerospace Information Report (AIR) 1751.[1] This AIR contains two equations, one used to compute attenuation from air-to-ground propagation (for airborne aircraft) and one for computing attenuation from ground-to-ground propagation (for aircraft taxiing, landing or in takeoff-ground roll). Up to and including INM Version 5.2,[2,3] these two field-measurement-based (empirical) equations have been used for computing lateral attenuation for all commercial aircraft within the model. Similar empirical equations have been used for military aircraft in INM.

Released in 1981, SAE AIR 1751 is based on data that was compiled in the 1960s and 1970s. The majority of the aircraft represented in this data set were equipped with low-bypass ratio jet engines. In addition, a single type of jet aircraft, the older Boeing Model 727-100 dominated the data set. It is generally recognized by the technical community that the SAE-based lateral attenuation algorithm within INM is the single-biggest ***acoustic*** weakness in the model for the following two reasons: (1) the algorithm, which represents a single relationship developed from data dominated by one type of aircraft, is applied equally to the entire fleet; and (2) the algorithm cannot account for propagation effects over acoustically hard terrain, a major weakness at airports in coastal areas. Consequently, in 1997 the INM development team initiated the task of revising the lateral attenuation algorithms within the model.

At the most fundamental level, the lateral attenuation of aircraft noise comprises two basic physical phenomena, engine installation effects and ground effects. Engine installation effects, which are implicit in the current SAE AIR 1751 algorithms, may account for sound reflections off of the aircraft wings and fuselage, and sound shielding primarily from the fuselage. In most cases, these effects are thought to be small (and possibly negligible) relative to ground effects. In fact, in the soon-to-be released updated version of the United States Air Force's NOISEMAP computer program for assessing noise impact in the vicinity of military installations, engine installation effects are neglected and lateral attenuation is based solely on ground effects.[4] However, the data that were used in the development of SAE AIR 1751 seem to indicate that for some commercial jet aircraft (e.g., the Boeing Model 727) engine installation effects may be important, depending upon source-to-receiver geometry. Figure 1 shows an example of measured lateral attenuation data for the 727, the theoretical ground effect curve for the 727 (discussed further herein), and the difference between the two (thought to be engine/aircraft installation effects). Because of the location of the engines on the 727 (i.e., fuselage/tail-mounted), associated installation effects are expected to be largest for this aircraft. Other aircraft with similar engine configurations for which the installation effect may be important include the McDonnell-Douglas Model MD80 and MD90 series aircraft. It is expected that for aircraft with wing-mounted engines, the installation effects will be much smaller, and possibly negligible[5]. The manner in which these installation effects will be accounted for in INM is currently under investigation. Because it is unclear how these installation effects will ultimately be accounted for (if at all), a before/after comparison of INM noise contours is not presented in this article. . Ground effects account for the introduction of an impedance boundary, in this case the ground surface, into a given aircraft-to-receiver geometry. This paper focuses on ground effect, which is the most substantial component of the lateral attenuation of aircraft noise.

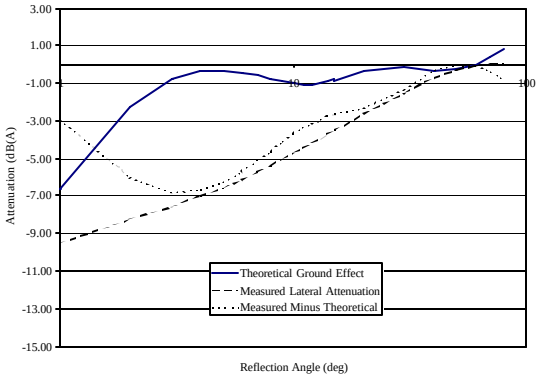

Figure 1. Example of Possible Engine/Aircraft Installation Effect

The new approach for computing ground effects in INM, described in detail herein, is founded in acoustic theory and has undergone rigorous laboratory and field tests. A recently-completed field study at Denver International Airport shows that predicting ground effects using the theoretical model described herein offer a substantial improvement over predicting ground effects with the equations currently in SAE AIR 1751[6]. The improvement is as large as 5 dB at an emission angle of three degrees. An additional in-situ field test is underway at Boston's Logan International Airport to further examine the accuracy of this theoretical approach[7].

The specific methodology described herein does not include enhancements for undulating terrain, including undulating terrain that blocks the source-to-receiver line-of-sight, i.e., barrier effects. The effects of undulating terrain are currently being evaluated in an effort to reach an acceptable compromise between accuracy and runtime. It is likely these effects will be included in a future version of INM.

Ultimately, it is the intent of the INM development team to have the ***general*** lateral attenuation approach peer-reviewed by the SAE A-21 Committee on Airport Noise, and approved for publication as a replacement to SAE AIR 1751. In fact, for the past year the development team has been briefing A-21 on the progress of the work. In general, this effort has been looked upon quite favorably by the technical committee. At a recent A-21 meeting[8], members of the development team volunteered to prepare a draft replacement of SAE AIR 1751 with the ground effects concept based on the general methodology described herein, along with possible consideration for the engine/aircraft installation effect, if deemed appropriate.

2. REFERENCE SPECTRAL DATA

The starting point in any empirical model such as INM is a reference data base. In Version 5.2 and in previous versions, the reference data base consisted solely of a set of noise level data expressed as a function of aircraft power and aircraft-to-receiver distance (i.e., noise-power-distance [NPD] data). The noise level data exist as either an exposure-based descriptor (i.e., A-weighted sound exposure level or effective perceived noise level, L_{AE} or L_{EPN}) or a maximum sound-level descriptor (i.e., maximum A-weighted sound level with slow exponential time weighting or maximum tone-corrected perceived noise level with slow exponential time weighting,

L_{ASmx} or L_{PNSmx}). To accurately account for overground propagation effects, this noise level data had to be supplemented with frequency-based data at some level of detail. This requirement is because overground propagation effects are a relatively complex function of frequency.

Reference 9 presents spectral data for a majority of the civilian aircraft included within INM. For each aircraft, this report presents the one-third octave-band spectrum measured at the time of L_{ASmx} and corrected to a distance of 1000 ft, assuming the SAE AIR 1845[10] atmospheric absorption coefficients. Similar data for the military aircraft in INM were provided by the United States Airforce.[11] These data also exist in the form of one-third octave-band spectra measured at the time of L_{ASmx} and corrected to a distance of 1000ft, assuming the SAE AIR 1845 atmospheric absorption coefficients. In addition, the raw data from previous Volpe Center helicopter noise measurement studies were reprocessed to obtain the one-third octave-band spectrum corrected to the same conditions as above. Note that these referenced helicopter noise measurement studies are the source of the NPD data which currently reside in FAA's Heliport Noise Model (HNM) Version 2.2.[12] Although helicopters likely will not be included in INM in the near-term, such data were easily added to the scope of the development and are included in the discussion herein for completeness.

Although the above references included spectral data for the majority of INM aircraft, the data were not available for 14 aircraft, which were mostly older models. For this reason it was decided that supporting a separate spectrum for each INM aircraft was not feasible. Based on sensitivity tests, it was also determined that maintaining separate spectral data for each aircraft would result in a negligible improvement in computational accuracy. Consequently, the approach of grouping similar spectra seemed to offer a logical compromise.

As a result, an exhaustive set of sensitivity tests (as discussed below) was conducted to identify spectra which could be grouped together, referred to herein as a ***spectral class***, resulting in the introduction of a negligible error in ground effects (as a result of the simplification associated with the grouping). Aircraft were first grouped together by engine type and/or number of engines (i.e., low-bypass ratio jet, high-bypass ratio jet, four engine jet, turboprop, piston, etc.), and then the groups were broken down further by spectral shape. Once the spectra were grouped together, a representative spectrum was detemined for the group. The representative spectrum for commercial aircraft was determined considering operational information contained in the 1995 national operational data base[13]; and the representative spectrum for military aircraft was determined considering 1997 fleet inventory data[14]. The ground effect for each aircraft in the group was then computed to be certain that the ground effects at all angles and distances of interest (0.1 to 20 degrees and 200 to 6000 m) were similar. These sensitivity tests indicated that the ground effects computed with the representative spectrum, as compared with that computed for the other spectra in a given class, were generally within ±1 dB of one another, although in a few instances deviations as large as ±3 dB were observed (Note: these larger deviations were only observed for aircraft which are not in widespread use (e.g., McDonnell Douglas DC-6, Convair 340, Mitsubishi MU300)).

INM contains 72 unique spectral classes. In total, there are 31 classes for departure, 34 classes for approach, and 7 classes for level flyover (applicable to helicopters only). As an example, the INM aircraft included within Departure Spectral Class 101 include the 727, 737 and DC-9 with the older Pratt and Whitney JT8D series engines, the DC10 with the General Electric CF6 series, L1011 with the Rolls Royce series RB2112 engines, and the F100 with the TAY620 and TAY 650 series engines. Figure 2 presents the individual spectra, along with the representative spectrum, for Departure Spectral Class 101.

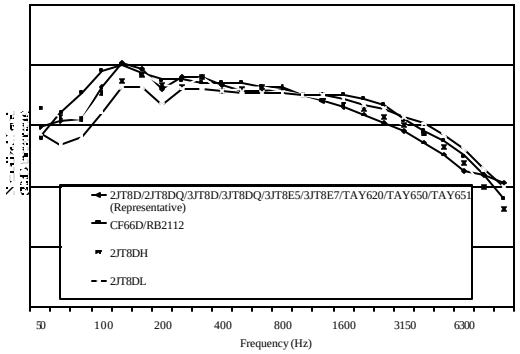

Figure 2. Departure Spectral Class 101

3. GROUND EFFECTS MODEL

The ground effects model documented by Tony **E**mbleton, Joe **P**iercy and Giles **D**aigle (the EPD Model) of the National Research Council (NRC) of Canada is the scientific foundation for the updated ground effects equations slated for inclusion in INM. The EPD model is documented extensively in References 15 through 17. Consequently, a brief overview is all that is presented herein. It is important to point out, however, that the EPD model is an assemblage of acoustic research which dates back to the works of Ingard in the 1950s.[18] The derivative work most germane to the discussion presented herein is that of Delany and Bazley, and Chessell.[19,20] It is also important to note that there are other ground effects models which are based on an assemblage of similar and/or identical research conducted over the years.[21-23] Many of these models will generate identical results to those computed by the EPD model, primarily because they are based on the above-referenced works of Delany, et. al. Because of the extensive field measurement validation, performed at various values of effective flow resistivity, for source heights up to 1.8 m, receiver heights up to 1.5 m, and source-to-receiver distances up to 1097 m, conducted in support of its development[15,16], the EPD implementation of this compilation of work was selected for INM development.

The ***basic*** EPD model relies Equation 1, which defines the sound pressure, p, at a receiver positioned above a ground surface, as in Figure 3.

$$\frac{p}{p_0} = \left\langle \left(\frac{e^{ik_1 r_1}}{k_1 r_1} \right) \right\rangle + \left\langle R_p \left(\frac{e^{ik_1 r_2}}{k_1 r_2} \right) + \frac{(1 - R_p) F(\omega) e^{ik_1 r_2}}{k_1 r_2} \right\rangle \quad [1]$$

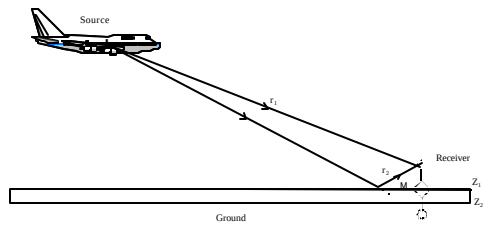

Figure 3. Generic Geometry for EPD Model

In Equation 1, the first term on the right-hand side of the equality represents the pressure associated with the direct source-to-receiver sound wave, and the second and third terms combined represent the pressure associated with the ground-reflected source-to-receiver sound wave.

The plane-wave reflection coefficient, R_p, in Equation 1 is computed as follows:

$$R_p = \frac{\left[Z_2 \sin\phi - Z_1 \left(1 - \left(\frac{k_1^2}{k_2^2} \right) \cos^2\phi \right)^{1/2} \right]}{\left[Z_2 \sin\phi + Z_1 \left(1 - \left(\frac{k_1^2}{k_2^2} \right) \cos^2\phi \right)^{1/2} \right]} \qquad [2]$$

In addition, the complex ground wave function, F(T) is computed as follows:

$$F(\omega) = 1 + i\pi^{1/2}\omega^{1/2} e^{-\omega} + \mathrm{erfc}\left(-i\sqrt{\omega}\right) \qquad [3]$$

Where: erfc is the complimentary error function.

In Equations 1 through 3: p is the sound pressure; p_0 is the sound pressure at a reference distance of 1m; k_1 and k_2 are the wavenumbers of the sound-field in air and in the ground surface, respectively, given by 2B/wavelength; r_1 and r_2 are the source-to-receiver distance associated with the direct wave and the ground-reflected wave, respectively; Z_1 and Z_2 are the specific acoustic impedance of air and of the ground surface, respectively; N is the angle (in two dimensions) between the ground-reflected ray and the ground surface; and T is the numerical distance given by the following equation:

$$w = i\frac{2k_1 r_2}{(1 - R_p)^2}\left(\frac{Z_1}{Z_2}\right)^2\left(1 - \frac{k_1^2}{k_2^2}\cos^2 f\right) \qquad [4]$$

Delany and Bazley[19] have developed equations for the specific acoustic impedance, $Z_2=R_2+iX_2$, and wavenumber $k_2="_2+i\$_2$, of acoustically absorptive surfaces, such as a typical ground surface. These equations are as follows:

$$\frac{R_2}{\rho_1 c_1} = 1 + 9.08\left(\frac{f}{\sigma}\right)^{-0.75}$$

$$\frac{X_2}{\rho_1 c_1} = 11.9\left(\frac{f}{\sigma}\right)^{-0.73}$$

$$\frac{\alpha_2}{k_1} = 1 + 10.8\left(\frac{f}{\sigma}\right)^{-0.70}$$

$$\frac{\beta_2}{k_1} = 10.3\left(\frac{f}{\sigma}\right)^{-0.59} \qquad [5]$$

In the above Delaney and Bazley equations (identified as Equation 5): D_1c_1 is characteristic impedance of air; f is frequency; and F is the effective flow resistivity of the ground surface expressed in cgs rayls. The effective flow resistivity used in the development of INM was either 150 rayls for acoustically soft ground (typical of field grass) or 20,000 rayls for acoustically hard ground (typical of water or pavement). For consistency with the EPD model, the sign in the above equation for the term X_2/D_1c_1 was changed as compared with that included in the original Delany and Bazley reference.

Figure 4 presents an example of the acoustically soft ground effect as a function of frequency for a rather simple source-to-receiver geometry (source height=0.31 m; receiver height=1.2 m; and source-to-receiver distance=15.2 m). Similar figures are presented in References 15 through 17 for various source-to-receiver geometries. To ensure proper implementation of the model, the data presented in these published graphics were all verified separately with the version of the EPD model implemented in support of INM development.

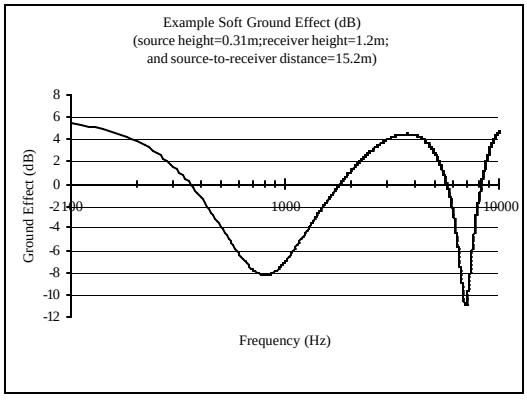

Figure 4. Example Computations for EPD Model

4. GROUND EFFECTS DATA BASE

The library of spectral class data provided the reference data base for computing overground propagation effects. It was determined that implementing the EPD model directly into INM would dramatically increase run-times by a factor deemed unacceptable in practice. Tests showed that fitting a series of regression equations to the ground effects data would result in more reasonable run-times. For the regression analysis, the spectral data along with the EPD physical acoustics model discussed above were used in tandem to develop a comprehensive ground-effect data base. The process used for developing the ground-effects data base is discussed in detail below.

As shown in Figure 5, the following steps are performed for a given source to receiver geometry, ground type, (i.e., acoustically hard or soft, flow resistivity of 20,000 rayls or 150 rayls, respectively), and frequency weighting (A-weighting and C-weighting are planned for final incorporation into the INM; and for the tone-corrected perceived noise descriptors in INM, e.g., L_{EPN}, computations based on A-weighting will be utilized).

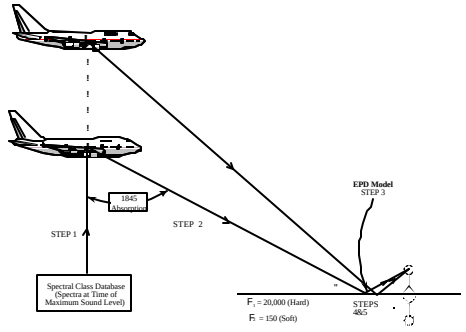

Figure 5. Overview of Process for Developing Ground Effects Data Base

1. The spectrum for a given class (representative of a spectrum at the time of L_{ASmx}, at a distance of 305 m, adjusted for frequency weighting) was corrected back to the source taking into account the effects of atmospheric absorption over the 305 m distance, by assuming the SAE AIR 1845 atmospheric absorption coefficients.

2. The source-corrected spectrum was then corrected to the point of specular reflection on the ground (the point of specular reflection is based on a 1.2 m microphone height -- other microphone heights are planned for final incorporation into the INM), again taking into account the effects of atmospheric absorption associated with the SAE AIR 1845 atmospheric absorption coefficients.
3. The corrected spectrum was then adjusted for ground effects using the computations of the EPD model. (Namely, the EPD model was run for the specific geometry, and programmed to compute a ground effect for 21 logarithmically-spaced frequencies within each one-third-octave band from 50 Hz to 10 kHz, beginning at the Base-10 lower edge of each one-third-octave band, e.g., 891.25 Hz for the 1 kHz one-third-octave band. The ground effect for a given one-third octave band was then computed by simply linearly averaging the 21 ground effect values within a given band. Although sensitivity tests showed that computing ground effect for more than three logarithmically-spaced frequencies typically resulted in a negligible improvement in accuracy, the 21-frequency approach was utilized to ensure the highest level of accuracy, and resulted in no negative effects since computer runtime was not an issue.).
4. The individual SPL values in each band of the corrected spectrum were then summed on an acoustic energy basis before and after step 3.
5. The decibel values computed in Step 4 were then arithmetically subtracted (after application of EPD minus before application of EPD). The difference between these two decibel values represents the ground effect. A negative ground effect indicates attenuation, and a positive ground effect indicates an increase in level.

Steps 1 through 5 were repeated for each of the following source-to-receiver distances: 200, 400, 630, 1000, 2000, 4000 and 6000 meters; and for 32 increments of reflection angle from 0.1 to 85 degrees. The incremental spacing of the reflection angle was selected to most accurately represent the behavior of the ground effect for a typical aircraft geometry (i.e., the 32 angles selected were as follows: 0.1, 0.2, 0.3, 0.4, 0.5, 0.6, 0.7, 0.8, 0.9, 1, 2, 3, 4, 5, 6, 7, 8, 9, 10, 11, 12, 13, 14, 15, 20, 30, 40, 50, 60, 70, 80, and 85 degrees). In all cases a receiver height of 1.2 m was assumed (other receiver heights are planned for final incorporation into the INM).

The result of the above process is a ground effects data base (i.e., a table of ground effects values), existing as a function of source-to-receiver distance and reflection angle.

5. REGRESSION ANALYSIS

The next step in the process is to accurately represent the ground effect database with a set of regression curves (or underlying regression equations). A fairly comprehensive statistical analysis was undertaken to determine the functional form of the regression equation(s) that would best represent the computed database. Specifically, previous work[24,25] indicated that the overground propagation effect was best described simply by the two independent variables: reflection angle and source-to-receiver ground distance. Further inspection of the data indicated that a separate functional form should be used for each value of effective flow resistivity (i.e., acoustically soft ground with an effective flow resistivity of 150 and acoustically hard ground with an effective flow resistivity of 20,000). The statistical analysis package Statistica[26] was used throughout the analysis.

5.1 Acoustically Soft Ground Regression Analysis

Initially, a simple polynomial relationship was used for the soft ground regression, but a subsequent error analysis indicated that this was inadequate. Numerical experiments indicated that an increase in the accuracy of approximation could be achieved by adding an exponent to the reflection angle term. In addition, a free-field adjustment term was added to the equation, which effectively corrects the spectral data (to which the ground effect value will be applied), which were measured by a 1.2 m microphone over acoustically soft ground (typically during aircraft noise certification tests), to a free-field situation (Note: The adjustment to free-field conditions for each spectral class was arrived at by arithmetically averaging the EPD-based ground effect values at 30, 40, 50, 60, 70, and 80 degrees for source-to-receiver distances of 200, 400, 630, and 1000 m.) The functional form of the final regression used for acoustically soft ground is as follows:

$$A_{Soft} = FF_{ADJ}+\{X_1+X_2\,(.0031d)+(X_3)(.0031d)^2\}+ \{X_4+X_5\,(.0031d)+(X_6)(.0031d)^2\}\{0.1\,\theta\}^Y+ \{X_7+X_8\,(.0031d)+(X_9)(.0031d)^2\}\{0.1\,\theta\}^2 \ dB(A) \quad [6]$$

Where: A_{Soft} is the total ground effect in decibels (A-weighted) for a pure acoustically soft ground geometry; FF_{ADJ} is the free-field adjustment term (dB(A)); X_N and Y are empirically-derived regression coefficients; d is source-to-receiver ground distance (m); and θ is the reflection angle (degrees).

Calculation of the final regression coefficients was arrived at through an expansion of the traditional Least Squares methodology. To improve the accuracy of the computed regression equations, the initial range of reflection angles from 0.1 to 85 degrees was segmented into eleven sub-segments selected as follows: 0.1 to 0.4 degrees; 0.4 (inclusive) to 0.7 degrees; 0.7 (inclusive) to 1 degrees; 1 (inclusive) to 3 degrees; 3 (inclusive) to 4 degrees; 4 (inclusive) to 6 degrees; 6 (inclusive) to 8 degrees; 8 (inclusive) to 10 degrees; 10 (inclusive) to 15 degrees; 15 (inclusive) to 40 degrees; and 40 (inclusive) to 85 degrees. In subsegmenting the regression there was some concern about introducing discontinuities at the junction of the subsegments. Consequently, an analysis of discontinuities was performed at the junction of these subsegments. The result was that all discontinuities were less than 0.3 dB, with 95 percent less than 0.1 dB.

As an example, Figures 6 presents the original data in the ground effects data base (directly from the EPD model) along with the computed regression for propagation over acoustically soft ground for departure spectral class 101 and a distance of 1000 m. These comparisons can be considered typical.

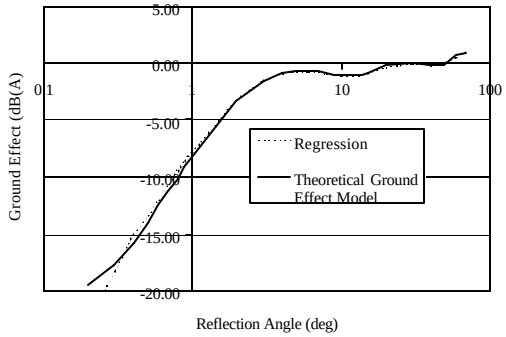

Figure 6. Comparison of Model Output and Regression Departure Spectral Class 101; Distance=1000 m; Acoustically Soft Ground

5.2 Acoustically Hard Ground Regression Analysis

An exponential relationship of the following form was used for the acoustically hard ground regression equation:

$$A_{hard} = FF_{ADJ}+(Q+(A/(1+e^{(B0+B1\log(\theta))})))*(C0+C1*d)\ dB(A) \quad [7]$$

Where: A_{Hard} is the total ground effect in decibels (A-weighted) for a pure acoustically hard ground geometry;FF_{ADJ} is the free-field adjustment term (dB(A)), as discussed in detail in Section 5.1; Q, A, B0, B1, C0, and C1 are empirically-derived regression coefficients;d is the source-to-receiver ground distance (m); and,θ is the reflection angle (degrees).

As an example, Figure 7 presents the original data in the ground effect data base (directly from the EPD model) along with the computed regression for propagation over acoustically hard ground for departure class 101 and a distance of 1000 m. These comparisons can be considered typical.

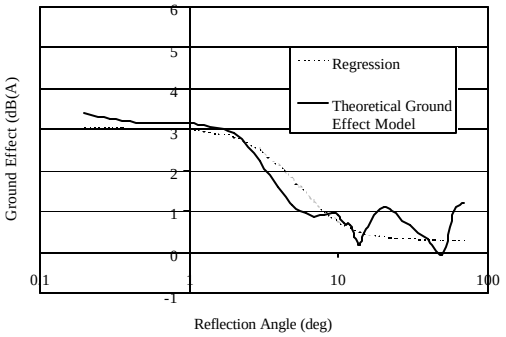

Figure 7. Comparison of Model Output and Regression Departure Spectral Class 101; Distance=1000 m; Acoustically Hard Ground

6. IMPLEMENTATION OF REGRESSION EQUATIONS

Before the regression equations could be implemented within the INM, several practical constraints had to be incorporated into the design. Most of these constraints were specific to the effective flow resistivity of the ground surface, and as such are discussed separately for acoustically soft ground and acoustically hard ground, respectively, in Section 6.1 and 6.2.

One general implementation issue has to do with modeling of non-departure and non-approach operations within INM. Specifically, INM supports several types of operations beyond just departures and approaches. For example, the INM user is allowed to define overflights, circuits, runups and touch-and-gos. At this time, unique spectral data do not exist for these types of operations. Therefore, for implementation within INM, overflights, circuits, runups and touch-and-gos are evaluated using the appropriate departure spectral class.

Additionally, for the purpose of computing ground effect, a nominal ***source*** height was set when the aircraft was on the ground. The nominal source height was 6.1 m for large jets, 1.524 m for small jets and propeller driven aircraft and 3.1 m for helicopters. These heights were arrived at through examination of representative scaled photographs of the more common models of aircraft within each of the three categories.

6.1 Acoustically Soft Ground Constraints

A limit of -20 decibels of total ground effect was placed on the acoustically soft ground equations. Practically, this limit will only be triggered at large source-to-receiver distances when the aircraft is on the ground, and the ground surface is acoustically soft. The -20 decibel limit was selected because in situations where this limit would be reached (i.e., shallow incidence angles and ground-to-ground propagation), atmospheric effects, including turbulence, tend to be the most significant propagation phenomena, effectively masking any ground effects.[27]

The EPD model was sometimes found to behave counter-intuitively at extremely large source-to-receiver distances (i.e., greater than 4000 m) and small angles (i.e., grazing angles) for propagation over acoustically soft ground. To eliminate this behavior, a large distance cutoff of either 4000 or 6000 m (depending on spectral shape), and a small angle cutoff of 0.1 degrees was applied. Distances larger than the imposed cutoff were evaluated at the cutoff distance, and angles smaller than the imposed cutoff were evaluated at the cutoff angle. This counter-intuitive behavior is exemplified in Figure 6 for reflection angles below about 0.5 degrees.

In addition, the small variation in the acoustically soft-ground effect for the larger reflection angles (as exhibited in Figure 6 for angles above about 30 degrees), although considered physically realistic and supported somewhat by the literature,[28,29] was considered impractical to represent in the final implementation for several reasons: (1) random variations in ground effect of +/- 0.5 dB about a mean value are bounded by the accuracy associated with the spectral class groupings, and are therefore considered insignificant; (2) acoustically soft-ground effects are generally considered to be negligible for reflection angles greater than about 20 degrees;[30] (3) the NPD data in the data base of the INM should be minimally affected by acoustically soft ground for elevation angles resembling those encountered at a centerline microphone during aircraft noise certification.[31] (In other words, there should be an inherent consistency between aircraft noise certification data and the INM NPD data.); and (4) not evaluating the regression equation for large reflection angles will dramatically improve INM runtime.

Consequently, it was decided that the acoustically soft-ground regression equations would not be invoked for reflection angles of 30 degrees and above; and for angles below 30 degrees an increase in sound level due to acoustically soft ground would not be allowed. To ensure these restrictions did not introduce a discontinuity in the ground effect at 30 degrees, the actual regression equations were truncated at 20 degrees and a simple linear function which converged to 0 dB at 30 degrees was substituted for the regression equations at angles between 20 and 30 degrees. In general, the ground effect at an angle of 20

degrees (where the linear function was initiated) was between 0 and -0.5 dB. The net result of this constraint is that acoustically soft ground can only reduce the computed sound level in INM, as opposed to increasing the level. In most cases, the acoustically soft-ground effect curve converged to zero at reflection angles between 5 and 20 degrees, depending upon aircraft type and source-to-receiver geometry, and therefore the 30 degree cutoff is rarely triggered.

6.2 Acoustically Hard Ground Constraints

As stated in Section 6.1, the EPD model was sometimes found to behave counter-intuitively at extremely large source-to-receiver distances and small angles for propagation over acoustically soft ground. Although this same behavior was not observed in propagation over acoustically hard ground, a large distance cutoff of 6000 m, and a small angle cutoff of 0.1 degrees was applied, to eliminate any possibility that counter-intuitive behavior would occur at distances and angles that were not tested. Distances larger than the imposed cutoff were evaluated at the cutoff distance, and angles smaller than the imposed cutoff were evaluated at the cutoff angle.

A decrease in sound level due to acoustically hard-ground, although considered physically realistic, was considered impractical to represent in the final implementation. In addition, an increase in sound level greater than 6 dB is physically unrealistic and was not allowed.

6.3 Application for Mixed Ground

The regression coefficients, along with the above mentioned constrains, were implemented in INM for acoustically soft and hard ground situations. However, many practical modeling situations include propagation over mixed, acoustically soft and hard terrain. Consequently, a methodology had to be developed to properly account for such situations. The approach decided upon was very similar to that implemented within the Federal Highway Administration's Traffic Noise Model (FHWA TNM ®)[28,29] and is based on the work of Boulanger.[32] Specifically, the acoustically soft-ground and hard-ground effect were apportioned based on a distance-weighted coefficient. This coefficient was computed based on the ground distance associated with the acoustically hard and acoustically soft portion of the ground contained within the so-called Fresnel Ellipsoid. The Fresnel Ellipsoid is a frequency-dependent function used fairly extensively in acoustics. The nature of the function is such that the ellipsoid effectively widens for lower frequencies and narrows for higher frequencies. The relationship is made to be consistent with the relationship between the frequency of a sound and its wavelength. In the most thorough approach, the portion of each ground type contained within the Fresnel Ellipsoid would be computed, and the ground effect would be apportioned out, at each of the 21 frequencies within each one-third octave-band. This approach is computationally intensive; therefore a simplification has been developed. In the simplified approach, the ellipsoid is computed for an effective frequency, and the resultant apportioning is performed on the total ground effect. The effective frequency is selected to best replicate results if the Fresnel based ellipsoid were computed for each one-third octave-band. An effective frequency of 44 Hz (the lower bandedge of the 50 Hz one-third-octave band) was chosen for initial implementation. The choice of an effective frequency of 44 Hz results in a relatively large ellipsoid, which takes into account a substantial area in the vicinity of the point of specular reflection. Provisions have been made within INM such that this frequency can be easily refined in the future if deemed appropriate.

As an example of a mixed ground implementation (see Figure 8), given a source-to-receiver ground distance of 1000 m, where the first 700 m of propagation is water (acoustically hard) and the remaining 300 m is grass (acoustically soft):

For example (see Figure 8), given a source-to-receiver ground distance of 1000 m, where the first 700 m of propagation is water (acoustically hard) and the remaining 300 m is grass (acoustically soft):

(1) the appropriate regression is evaluated assuming a pure acoustically soft situation;

(2) the appropriate regression is evaluated assuming a pure acoustically hard situation;

(3) the ground effect computed in Steps 1 and 2 for acoustically soft and acoustically hard ground, respectively, is combined in accordance with the following equation:

$$A_{Hard/Soft} = \left(\frac{d_1}{(d_1 + d_2)}\right) A_{Hard} + \left(\frac{d_2}{(d_1 + d_2)}\right) A_{Soft} \quad dB(A) \qquad [7]$$

Where: $A_{Hard/Soft}$ is the total ground effect in decibels for a mixed acoustically hard and soft geometry; d_1 is the acoustically hard portion of the ground contained within the Fresnel Ellipsoid; A_{Hard} is the total ground effect computed assuming a pure acoustically hard ground situation; d_2 is the acoustically soft portion of the ground contained within the Fresnel Ellipsoid; and A_{Soft} is the total ground effect computed assuming a pure acoustically soft ground situation.

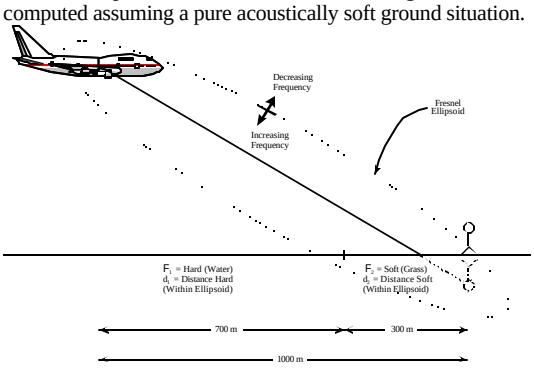

Figure 8. Example Geometry for Mixed Acoustically Hard and Soft Ground

7. REFERENCE HYDROGRAPHIC DATA

As part of the final implementation, a mechanism had to be developed within INM to facilitate automated input of acoustically hard terrain that was classified as such due to water cover, i.e., automated input of hydrographic data. The first step in this development was to establish a standardized file format for defining hydrographic objects such as lakes and rivers. This file format was set-up to include information on grid origin, grid spacing, grid size and the acoustic properties of the terrain polygons and lines (hydrographic objects) within the grid.

There are of course a plethora of sources for raw hydrographic data. One option, and probably the best in terms of accuracy, would be digitized information generated from maps or aerial photographs. This approach will obviously require a substantial amount of work on the part of the INM user. In some instances it may also leave the user in a quandary as to how to classify certain areas of land. For example, should an open area which is marshland in the spring, and dried-up field grass in the summer be classified as acoustically hard or acoustically soft? As a result, a more automated approach has been developed. A stand-alone

program, entitled "USGS" reads either singular or multiple contiguous United States Geological Survey (USGS) 1:100,000-scale digital line graph hydrographic files and automatically converts them into the standard INM file format. If deemed appropriate, the user has the option to augment the converted USGS data with acoustically hard areas that would not otherwise be included in the USGS files, e.g., large parking lots, or expansive highway systems. The particular hydrographic objects included in the USGS files are too numerous to mention (included are over 80 types), but they include areas (i.e., polygons), such as lakes and ponds, boundaries (i.e., lines), such as shorelines, and line segments such as rivers, and streams. The USGS data are available online at *http://edcwww.cr.usgs.gov/glis/hyper/guide/100kdlgfig/states.html* or through the USGS National Cartographic Information Center, User Services Branch, 507 National Center, Reston, Virginia 22092. Viewer programs for the USGS data are also available online at *http://mcmcweb.er.usgs.gov/viewers*.

A second stand-alone supporting program, entitled "HYDRO", converts the standard hydrographic file into a binary file of acoustically hard and acoustically soft, regularly-spaced grid points. This file has a simple header which contains grid size, resolution, and registering information, along with a grid of "1s" and "0s", where "1s" represent acoustically hard ground and "0s" acoustically soft. The specific resolution of the grid is user selectable. The grid file is used directly by INM to determine the percentage of acoustically hard and acoustically soft ground in a given source-to-receiver cross section.

Within INM, the ground projection from the microphone to a particular flight segment is effectively overlayed on the grid file. If the projection traverses acoustically hard or soft ground only, the appropriate ground effects regression equation is evaluated. If the projection traverses acoustically mixed grounds, the INM determines the appropriate percentage of acoustically hard and soft ground distances, using Equation [7] in Section 6.3.

8. CONCLUSION

This paper summarizes a scientifically based, experimentally validated methodology for computing ground effect within the FAA's INM. It will result in an improvement in the model's predictive accuracy, especially at small reflection angles. Further, it provides the INM user with the ability to take into account the effects of an acoustically hard surface such as water, including the effects of mixed, acoustically soft and hard ground surfaces, a capability never before available in the model. Recent field studies have shown the approach to agree well with measured data. Additional in-situ field tests will provide further validation of this model. However, more research will be needed in the future before engine installation effects are fully understood and can be incorporated into the model.

REFERENCES

1. Society of Automotive Engineers, Committee A-21, Aircraft Noise, Prediction Method for Lateral Attenuation of Airplane Noise During Takeoff and Landing, Aerospace Information Report No. 1751, Warrendale, PA: Society of Automotive Engineers, Inc., March 1981.
2. Olmstead, Jeffrey R., et.al., Integrated Noise Model (INM) Version 5.1 User's Guide, Report No. FAA-AEE-96-02, Washington, D.C.: Federal Aviation Administration, December 1996.
3. Fleming, Gregg G., et.al., Integrated Noise Model (INM) Version 5.1 Technical Manual, Report No. FAA-AEE-97-04, Washington, D.C.: Federal Aviation Administration, December 1997.
4. Speakman, J.D., "Lateral Attenuation of Military Aircraft Flight Noise", AAMRL-TR-89-034, July, 1989.
5. Soeiety of Automotive Engineers, Committee A-21, Aircraft Noise, Estimation of One-Third-Octave-Band Lateral Attenuation of Sound From Jet-Propelled Airplanes, Aerospace Information Report No. 1906, Warrendale, PA: Society of Automotive Engineers, Inc., February 1991.
6. Plotkin, Kenneth J., Hobbs, Christopher M., Bradley, Kevin A., "Examination of the Lateral Attenuation of Aircraft Noise", Wyle Research Report WR 99-10, Wyle Laboratories, Arlington VA, April 1999.
7. Fleming, Gregg G., Senzig, David A., Clarke, John-Paul, "Aircraft Noise Prediction Model Support", John A. Volpe National Transportation Systems Center Acoustics Facility Reimbursable Agreement with NASA Langley Research Center, July 1998.
8. Fleming, Gregg G., Rapoza, Amanda S., Burstein, Joseph, Senzig, David A., "Updated Lateral Attenuation for INM", Presentation to SAE Committee A-21 in Toulouse France, October 1998.
9. Bishop, Dwight E., Beckman, Jane M., Bucka, Mike P., Revision of Civil Aircraft Noise Data for the Integrated Noise Model (INM), Report 6039, Canoga Park, CA: BBN Laboratories Incorporated, September 1986.
10. Society of Automotive Engineers, Committee A-21, Aircraft Noise, Procedure for the Computation of Airplane Noise in the Vicinity of Airports, Aerospace Information Report No. 1845, Warrendale, PA: Society of Automotive Engineers, Inc., March 1986.
11. Mohlman, Henry T., "USAF Noisefile Database", AL-OE-WP-TR-1998-004, February, 1998.
12. Fleming, Gregg G., Rickley, Edward J., Heliport Noise Model (HNM) Version 2.2 User's Guide, Report No. FAA-AEE-94-01, Cambridge, MA: John A. Volpe National Transportation Systems Center Acoustics Facility, February 1994.
13. Airport Activity Statistics of Certificated Air Carriers, Washington, D.C.: U.S. Department of Transportation Statistics, Office of Airline Information, December 1995.
14. Aerospace Source Book, Aviation Week & Space Technology, McGraw-Hill Companies, January 12, 1998.
15. Embleton, Tony F.W., Piercy, Joe E., Daigle, Giles A., "Effective flow resistivity of ground surfaces determined by acoustical measurements," J. Acoust. Soc. Am. Vol. **74**, No. 4, pp 1239-1243, 1983.
16. Embleton, Tony, F.W.,"Sound Propagation Outdoors -- Improved Prediction Schemes for the 80's," Noise Control Engineering Journal, Vol. **18**, No. 1, pp 30-39, 1982.
17. Embleton, Tony F.W., Piercy, Joe E., Daigle, Giles A., "Outdoor Sound Propagation Over Ground of Finite Impedance," J. Acoust. Soc. Am. Vol. **59**, No. 2, pp 267-277, February 1976.
18. Ingard, K.U., "A review of the influence of meteorological conditions on sound propagation," J. Acoust. Soc. Am. Vol. **25**, No. 3, pp 405-411, 1953.
19. Delaney, M.E. and Bazley, E.N., "Acoustical properties of fibrous absorbent materials," Appl. Acoust. Vol **3**, pp. 105-116, 1970.
20. Chessell, C.I., "Propagation of noise along a finite impedance boundary," J. Acoust. Soc. Am. Vol. **62**, pp 825-834, 1977.
21. De Jong, B.A., Moerkerken, A., van der Toorn, J.D., "Propagation of Sound over Grassland and over an Earth Barrier," J. Acoust. Soc. Am. Vol. **86**, No. 1, pp 23-46, 1983.

22. Engineering Science Data Unit (ESDU)' "The prediction of sound attenuation as a result of propagation close to the ground," ESDU pac A9436, London, England: ESDU, November 1994.
23. Slutsky, Simon, Bertoni, Henry L., Parallel Noise Barrier Prediction Procedure (three volumes), Cambridge, MA: Transportation Systems Center, June 1987.
24. Plovsing, Birger, Aircraft Sound Propagation over Non-Flat Terrain, Prediction Algorithms, Draft Report. Lyngby, Denmark: Danish Acoustical Institute, August 1993.
25. Plotkin, Kenneth J., Moulton, Carey L., Stusnick, Eric, Feasibility of Incorporation of Terrain Effects into NOISEMAP. Technical Note TN 92-5, Arlington, VA: Wyle Laboratories, October 1992.
26. Statistica Version 5.1 (five volumes), Tulsa, OK: StatSoft Corporation, 1995.
27. Sutherland, Louis C., Daigle, Gilles A., "Atmospheric Sound Propagation", Encyclopedia of Acoustics, Chapter 32, pp 341-365, 1997.
28. Anderson, Grant A., Lee, Cynthia S.Y., Fleming, Gregg G., Menge, Christopher W., FHWA Traffic Noise Model (FHWA TNM®), Version 1.0: User's Guide, Report No. FHWA-PD-96-009, Cambridge, MA: John A. Volpe National Transportation Systems Center Acoustics Facility, January 1998.
29. Menge, Christopher W., Rossano, Christopher F., Anderson, Grant A., Bajdek, Christopher J., FHWA Traffic Noise Model (FHWA TNM®), Version 1.0: Technical Manual, Report No. FHWA-PD-96-010, Cambridge, MA: John A. Volpe National Transportation Systems Center Acoustics Facility, February 1998.
30. Piercy, Joe E., Daigle, Giles A., "Sound Propagation in the Open Air," Handbook of Acoustical Measurements and Noise Control, New York: McGraw-Hill, Inc., 1991.
31. Federal Aviation Regulations, Part 36, Noise Standards: Aircraft Type and Airworthiness Certification, Washington, D.C.: Federal Aviation Administration, September 1992.
32. Boulanger, P., Waters-Fuller, Tim, Attenborough, Keith, Ming Li, Kai, "Models and Measurements of Sound Propagation from a Point Source over Mixed Impedance Ground," J. Acoust. Soc. Am., Vol 102, no. 3, pp. 1432-1442, 1997.
33.